ISSN 1330-3651 (Print), ISSN 1848-6339 (Online) https://doi.org/10.17559/TV-20210713124155
Original scientific paper

The Possibility of Using Wavelet Analysis to Describe Computer-Modelled Surfaces

Katarzyna RASZKA

Abstract: The paper presents the issue of computer modelling of the surface after machining. The *modelowanie_skr* program, whose operation is based on subtracting simple geometric solids from a flat surface to create a given structure, was used. A front-milled surface was modelled, and two types of wavelets were placed on it; then the obtained surface image and parameters of the 3d structure were compared. The comparison was extended to cases where the surface disturbance occurred. Four types of disturbances, with a variable percentage, were distinguished. Conclusions determined the usefulness of selected wavelets in computer modelling and changes of the surface along with the application of disturbances and wavelets on it.

Keywords: 3d measurements; computer modelling; milling; roughness; surface; wavelet

1 INTRODUCTION

Designing the technological process to obtain specific functional features of the surface is a difficult and labour-intensive procedure. Therefore, the ability to predict the behaviour of the workpiece during machining and obtained results is a frequently used facilitation [1]. Using 2d profilometric analysis, there is no special need to use such solutions because this kind of measurement is simple and quick to perform. However, obtaining a complete topographic picture can be complicated, time-consuming, and expensive. Therefore, methods of functional surface analysis, such as mathematical modelling of surfaces, are used.

In general, we can divide surface modelling into 2 groups - FEM methods in which numerical approach is used to design the whole process of cutting, and simpler programs to model only the surface after machining.

The first one is widely known and has been used in many studies. It allows obtaining lots of results from different groups, e.g., forces during cutting [2, 3], chip breaking [4], temperature [5, 6], residual stresses [7]. The process of modelling has been changing through years. Depending on the current state of knowledge and techniques, different approaches were used. Most solutions focus on applying the Lagrangian and Euler techniques. The first one tracks discrete material points [8], the second one tracks volumes of material rather than single points [9]. Euler techniques may cause difficulties obtaining reliable results, e.g., the right course of chip form, because their algorithms assume constant chip thickness. Lagrangian algorithms also have imperfections, but most of their problems can be solved by remeshing and adaptive meshing [10, 11]. FEM methods may be used for optimizing the cutting process, extending tool life, reducing the time process, but at the same time, they require specialist software, which is often expensive, requires more computing memory, and can be difficult to learn.

Programs in which only surfaces are modelled are typically cheaper and easier to use. An example of this kind of program may be, as used in this paper, program *modelowanie_skr*. The program functions in the Matlab environment (version R2007b in the presented work), but it is opened as a separate module, so it does not require in-depth knowledge. Basic operations that can be performed in the program are discrete/continuous modelling, folding and deformation of profiles/surfaces, and profilometer needle filtration of profiles/surfaces. The surface creation is done intuitively - similar to the real cutting process, some material is subtracted from a flat surface. What we control is a cutting tool, in this case, a simple solid: an ellipsoid, a cone, a torus. The shape is properly formed, duplicated, and cut from the cuboid, which is the input material. At each stage of modelling, there are many variables, which allows obtaining various types of surfaces.

The simplest analysis of the surface is the parametric analysis, during which the values of given surface parameters from different groups (height, spatial, hybrid, functions, related to segmentation [12]) are assessed. Such tests have already been performed, and it has been positively stated that it is possible to correctly reproduce the surface after treatment through the modelled surface using *modelowanie_skr* program [13]. In this work, one can find a broader description of the program's operation and research confirming its correct operation. In addition, the software was used in conference lectures, where the focus was on selected types of surfaces: after grinding [14], determined [15], random [16] and plateau [17].

In the current research, it was decided to study the application of wavelet analysis on computer-modelled surfaces. Wavelet analysis may be a tool for topography research. It allows to extract the data of surface/profile components [18], characterize the surface [19], filter out disturbances/irregularities in measurement [20-22], or it can be a tool for assessing the condition of the surface of the tool [23]. By definition, wavelets are functions generating orthonormal bases of the $L^2(R)$ space [24] due to the shifting and scaling operation. They derive their name from the characteristic "waving" - they are variable, and their runs are dominated by values close to 0. Only in small sections, they have noticeably different values. The basic task of wavelet analysis is the approximation of the studied phenomenon. The wavelet transform is similar to the Fourier transform. They both use a dot product, where one element is the function being examined, and the other is the kernel of the transformation. For wavelet analysis, it is a wavelet function, for Fourier's method, a sinusoidal function. Moreover, the Fourier transform is mainly good for frequency analysis of series of a stationary nature and finding the characteristics of global signals. These are features different from the wavelet method, in which local features are also often examined, and the conducted time-frequency analysis is used to study non-stationary series [25]. Wavelet analysis is based on the description of the investigated function by wavelet functions that are generated by the parent (basic) wavelet $\psi(t)$ through its translation and scaling (scaling function $\varphi(t)$). The basic wavelet meets the following assumptions:

- it has a zero mean value,
- it can take non-zero values only in a certain closed range - otherwise it is called a compact medium,
- its duration (frequency response) is finite,
- it is orthogonal, so it cannot be written as a linear combination of any remaining elements of the set [26].

So far, no studies combining the advantages of using wavelets and surface modelling have been conducted. In this work, simple software for modelling the surface with the occurring disturbances was used, and then the wavelet analysis was performed. Modelling is a mathematical tool that allows separating the effects of the cutting tool on the directions of operation of individual components of the cutting forces. This is possible thanks to the before mentioned parameters, which are a quantitative assessment tool. Modelling also can help in predicting the functional properties of the treated surfaces. It shows how the machining process should proceed without the need for many previous tests on real surfaces. As for the wavelets, they allow for extending the possibilities of a qualitative description of the surface. The requirements for surfaces are so high they should be analysed in many aspects, and the classical Gaussian analysis does not show all their features. Therefore, wavelet analysis may be a useful tool for surface analysis. The combination of modelling and wavelet analysis can provide a tool for qualitative description of any structures with distinguished (or superimposed) features occurring in different directions of the surface.

2 PARAMETERS

In the work, the surfaces after face milling were modelled. For this purpose, it was found that the shape of the torus would work best. In the program, this figure additionally has the option of changing the cross-section, from an ellipse to any designed and loaded. Using some approximation, the shape of the ellipse can successfully imitate the milled surface; however, in order to better reflect the shape of the cutting insert, the cross-section was changed to the one shown in Fig. 1.

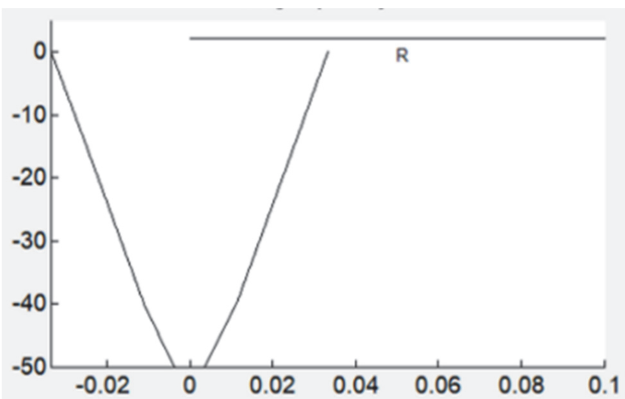

Figure 1 The shape of the cross-section of the torus

Selecting the right dimensions of the torus and the step of its shift, several surfaces were obtained, among which, due to the best compliance with the typical course of the milling head along the surface, it was decided to carry out further research on the surface presented in Fig. 2.

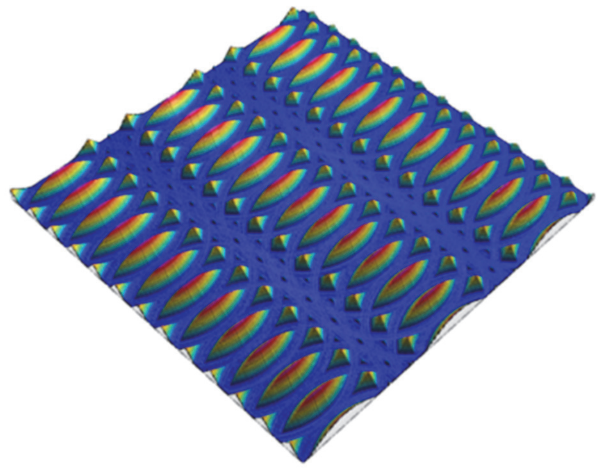

Figure 2 Image of the analysed surface (area 4 × 4 mm, highest point *Sp* = 25,63 μm, lowest point *Sv* = 4,24 μm)

The high concentration of traces in one axis and much less frequent on the other clearly illustrate the assumed movement of the tool along the surface.

Another factor that was taken into account during modelling was the size of the elements. Large dimensions of the torus were associated with the need to increase the area section, which significantly burdened the computer's memory and slowed down the modelling process. On the other hand, too small a section of the surface did not allow for a presentation of the right amount of details.

During modelling, there were 4 types of disturbances, which were introduced gradually, increasing their percentage value (Tab. 1). This resulted in 24 surface images with different disturbances and one original without any disturbances.

Table 1 Distortions of the surfaces

Type of disturbance	Subsequent values / %					
Shape of the cutting insert	1	2	3	4	5	6
Noise	0,5	1	1,5	2	2,5	3
High	5	10	15	20	25	30
Length	5	10	15	20	25	30

Among the wavelets available in the surface analysis software, two were selected to be applied to each surface: Daubechies 6 and Symlet 8.

The Daubechies family of wavelets is characterized by the compactness of the carrier with a length of $2N - 1$ (N is the row of wavelets), a relatively simple form and an exact approximation of a function. It is an extension of the Haar wavelet family [27]. Db1 means Daubechies of the first order. As the order of the wavelet increases, the number of coefficients describing it increases, and its course is smoother. Fig. 3 [28] shows the sixth order Daubechies used in the paper. The Symlet wavelet family is an extension of the Daubechies wavelets and was created by the Belgian mathematician Ingrid Daubechies as well. Symlet wavelets are almost symmetrical and show great similarity to their prototypes - Daubechies wavelets. Fig. 4 shows the eight order Symlet.

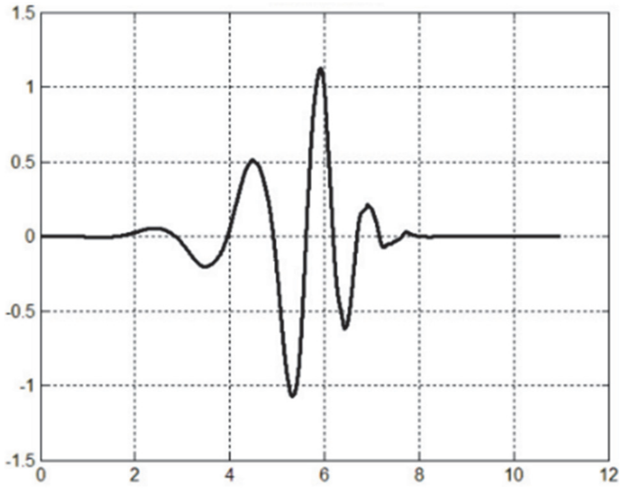

Figure 3 Daubechies 6 wavelet [26]

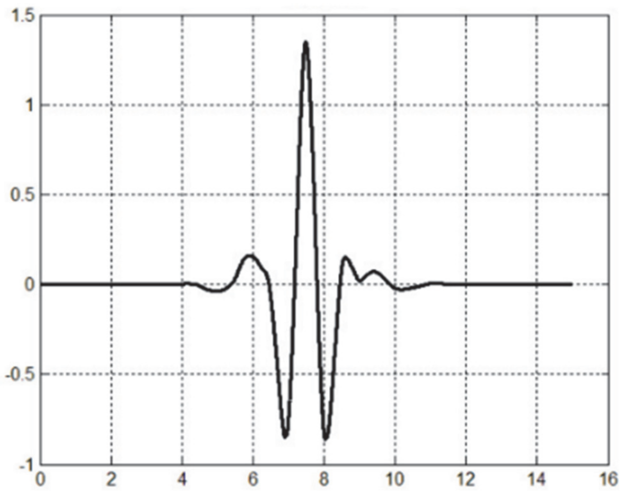

Figure 4 Symlet 8 wavelet [28]

Due to their characteristic shape, similar to the topography of the treated surface (good mapping of peaks and valleys), these two functions will be used in the presented work. Wavelets with such great similarity were selected in determining whether they can be used interchangeably or whether they will show differences in operation and, if so, how big the differences will be.

3 MEASUREMENTS

The measurements chapter of the paper is divided into 4 sections according to the type of disturbance. In each of them, the change of the surface image with the introduction of disturbances and wavelets and their influence on the obtained surface height parameters were considered.

3.1 Shape of the Cutting Insert Disturbance

The value of the deformation of the cutting insert shape was increasing 1% up to 6%, which was a critical value for maintaining the correct shape of the cutting insert, Fig. 5.

Six surface images were obtained, and the extreme one (6% disruption) is shown in Fig. 6. The surface images were analysed after applying the Daubechies 6, Symlet 8 wavelets (Fig. 7), and the height parameters of the surface: *Ssk*, *Sku*, *Sa*, *Sq*, *Sv*, *Sp*, *Sz*.

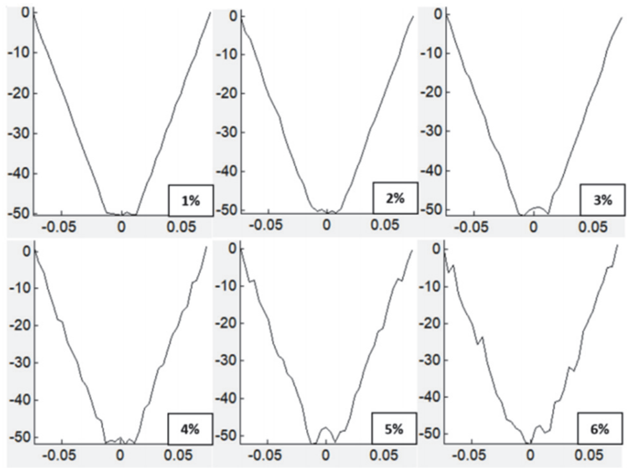

Figure 5 Shape of the cutting insert disturbance

Neither the noise of the plate nor the subsequent application of wavelets affected the general shape of the processing traces, which after introducing the disturbance became more jagged but still legible. The wavelets noticeably affected the area of the valleys between the successive passes of the tool, but still, the course of the milling head can be easily noticed in the form of periodically repeated surface irregularities.

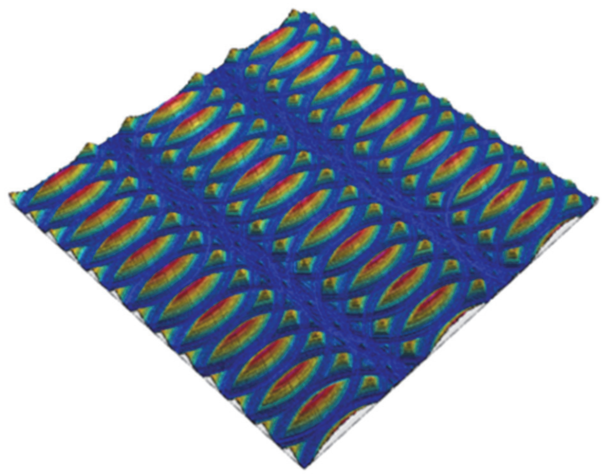

Figure 6 Surface with a 6% shape of the insert disturbance (area 4 × 4 mm, highest point *Sp* = 26,76 μm, lowest point *Sv* = 6,74 μm)

Fig. 7 presents the operation of the Db6 (top row) and Sym8 wavelets in extreme cases of disturbance (1% and 6%). Surface images show minimal differences in noise filtration. The action of both wavelets focused on the valley areas between successive passes of the tool, removing the traces of the tool passes resulting from the disturbance. Comparing both wavelets, the most "residue" after passes was left by the case of Sym8 with 6%.

The parametric analysis took into account the way of changing the values of subsequent parameters along with the disturbance increase, the behaviour of these changes when wavelet is applied, and the decrease/increase in the average values of the given parameters after the introduction of the wavelets.

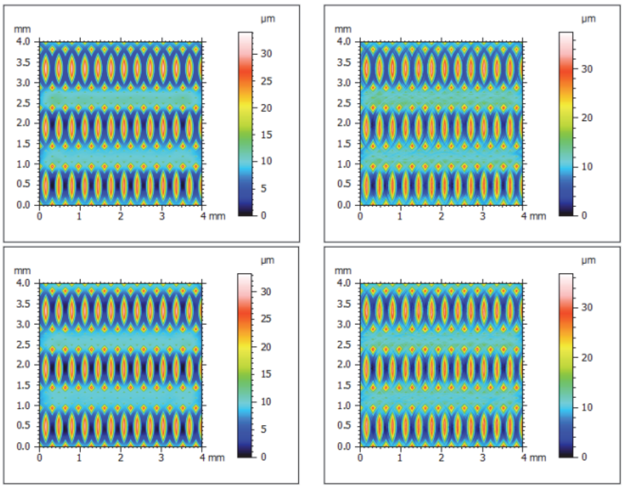

Figure 7 Surface images with 1% (left side) and 6% (right side) shape insert disturbance after using Db6 (top row) and Sym8 (bottom row) wavelets

During the analysis of the given parameters, two coefficients were used - the correlation and the significance of the change. In the tables, they are abbreviated as *r* - correlation coefficient and *p* - the significance of the change. Three conditions were adopted according to which the change of a given parameter was considered significant:

- correlation coefficient $r > 40\%$,
- *p* factor > 30% for values below 1,
- *p* factor > 8% for values above 1.

If any of the conditions have not been met (no correlation/small change in value), it has been marked in grey in the tables.

Table 2 Changes for the height parameters during the introduction of the disturbance in the shape of the insert and wavelets Db6, Sym8

	Increase/decrease			*r* / %			*p* / %		
	w/o	Db6	Sym8	w/o	Db6	Sym8	w/o	Db6	Sym8
Ssk	∨	∨	∨	90	90	91	18	21	21
Sku	∨	∨	∨	83	80	80	19	16	16
Sa	∧	∧	∧	82	85	86	12	14	14
Sq	∧	∧	∧	87	87	86	9	9	10
Sv	∧	∧	∧	98	94	100	59	38	25
Sp	∧	∧	∧	93	96	96	4	7	7
Sz	∧	∧	∧	100	98	99	12	16	12

Table 3 Changes for the *Sv* parameter during the introduction of the disturbance in the shape of the insert and wavelets Db6, Sym8

Sv / µm	Subsequent values / %						
	0	1	2	3	4	5	6
w/o a wavelet	4,24	5,08	5,44	5,78	6,11	6,43	6,74
Db6	9,13	10,79	11,15	11,49	11,84	12,22	12,6
Sym8	9,91	10,47	10,9	11,31	11,69	12,06	12,43

Tab. 2 presents a comparison of changes in parameters with the increase of the disturbance. The first column shows whether there has been an increase or decrease in the value of a given parameter with the introduction of a stronger disturbance. It can be seen that the nature of the course did not change with the introduction of wavelets, and the disturbance itself increases the values of most of the altitude parameters, except for those related to the ordinate distribution *Ssk, Sku*. The second column shows the correlation of changes in individual parameters. It can be seen that in all cases, there was a well-correlated course. The last column tells how much the increase/decrease in value occurred. The highest increase in value occurred for the parameter *Sv*, the course of which is additionally presented in Tab. 3. On the other hand, the smallest increase was the *Sp* parameter, where the changes were so small that they were considered insignificant.

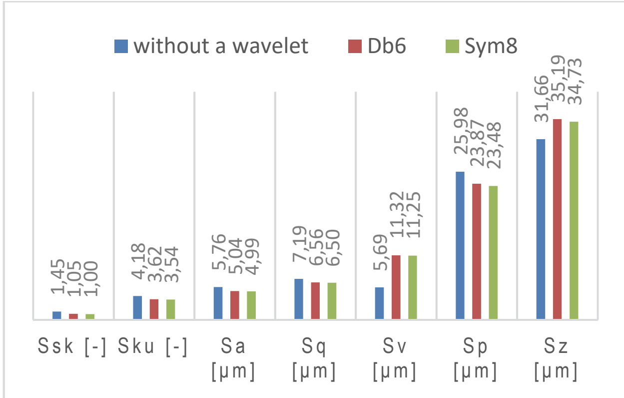

Figure 8 Averaged values of height parameters for surfaces without wavelets and surfaces with wavelets Db6 and Sym8

Fig. 8 presents a graph showing the change in average values with the introduction of wavelets. It shows that the wavelets cause a decrease in the value of most of the height parameters, with the exception of *Sv* and *Sz*, among which *Sv* is again distinguished (Tab. 3), whose increase is the highest.

3.2 Noise Disturbance

Another case of disturbance was the change in the noise value introduced on the entire surface, not locally on the insert. Fig. 9 presents changes in the appearance that occurred at the highest level of the introduced disturbance, 3%. In this case, even at low values, there were big changes in the appearance of the model, so it was changed every 0.5%. It can be seen that as the noise increases, the surface loses its original appearance and the original surface irregularities gradually disappear.

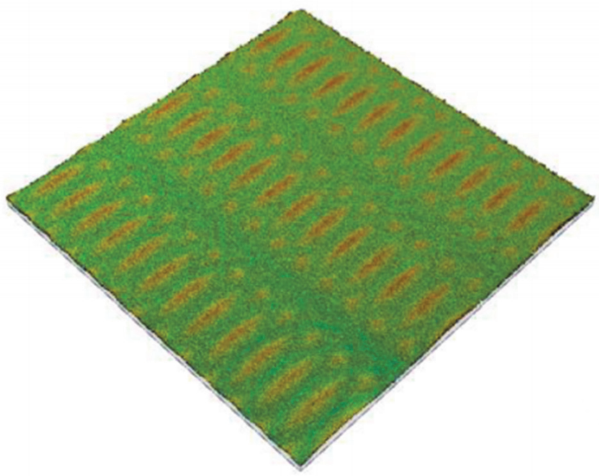

Figure 9 Surface with a 3% noise disturbance (area 4 × 4 mm, highest point *Sp* = 69,24 µm, lowest point *Sv* = 57,68 µm)

Fig. 10 shows what changes have occurred in the appearance of the surface after the introduction of Daubechies 6 and Symlet 8 wavelets on the surface with the lowest and the highest noise. Comparing the images, it can be seen that both of these wavelets gave very similar results. The level of the valleys between successive passages was raised, but the basic shape of the unevenness did not change.

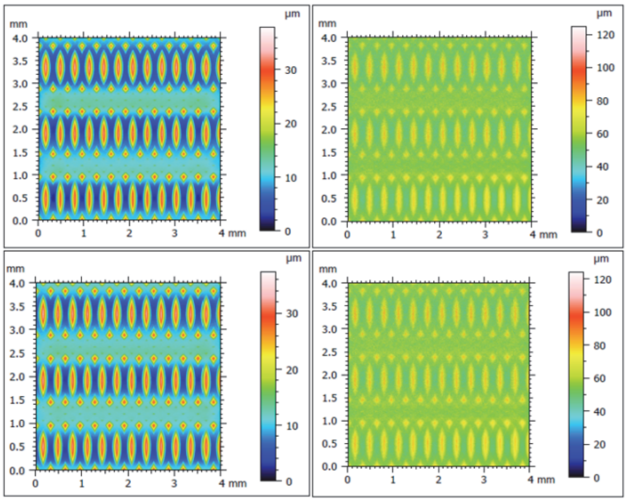

Figure 10 Surface images with 0,5% (left side) and 3% (right side) noise after using Db6 (top row) and Sym8 (bottom row) wavelets

Table 4 Changes for the height parameters during the introduction of the noise disturbance and wavelets Db6, Sym8

	Increase/decrease			*r* / %			*p* / %		
	w/o	Db6	Sym8	w/o	Db6	Sym8	w/o	Db6	Sym8
Ssk	∨	∨	∨	99	100	99	83	87	87
Sku	∨	∨	∨	97	97	90	33	22	20
Sa	∧	∧	∧	92	98	94	82	>100	>100
Sq	∧	∧	∧	93	99	93	81	92	84
Sv	∧	∧	∧	98	100	97	≫100	>100	>100
Sp	∧	∧	∧	97	99	97	>100	>100	>100
Sz	∧	∧	∧	97	100	97	>100	>100	>100

The changes caused by the introduction of surface noise (Tab. 4) follow a very similar course to the changes caused by the cutting insert shape noise. The main differences are focused on the scale of these changes. For example, again, the greatest increase in value was for the maximum plunge depth *Sv*, but this time there was more than a 10× increase between the initial value and the maximum value. In this case, all parameters changed strongly, except for *Sku*, which slightly decreased during the introduction of the disturbance.

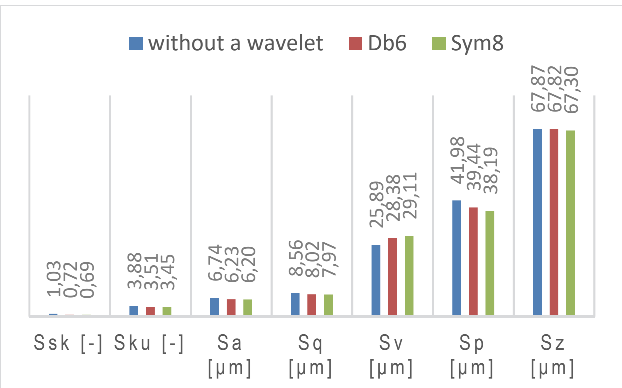

Figure 11 Averaged values of height parameters for surfaces without wavelets and surfaces with wavelets Db6 and Sym8

The diagram in Fig. 11 shows that most of the differences between the average values of the given parameters depending on the application of the Db6 and Sym8 wavelets are small and of a decreasing nature. We observe a slightly greater decrease in value for *Sp*, which is complementary to *Sv*, which in turn has the greatest increase between the absence of a wavelet and a Symlet wavelet.

3.3 Height Disturbance

In the case of disturbances in height and length, the disturbances were introduced every 5% up to 30%. Fig. 12 shows the surface with 30% height disturbance. Again, it did not change the basic shape of the inequality. The individual traces of the torus became clearer, and in several places they were more deeply sunk into the surface.

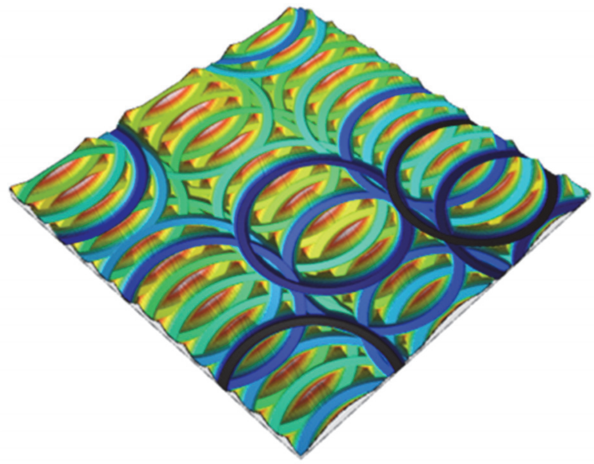

Figure 12 Surface with a 30% heigh disturbance (area 4 × 4 mm, highest point *Sp* = 29,78 µm, lowest point *Sv* = 18,82 µm)

Comparing the images with the use of wavelets (Fig. 13), it can be noticed that they managed to partially remove the changes resulting from the disturbance, but left a few places with clearly darker areas in which the effect of the disturbance was not reduced. In the central area of the images with 30% interference, the wavelet Db6 focused strongly on one segment of the torus, causing a large change in height there, while Sym8 introduced a more delicate change on a larger area of the torus.

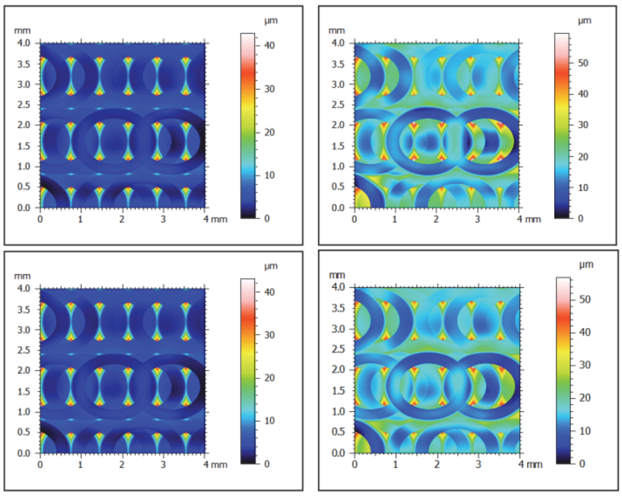

Figure 13 Surface images with 5% (left side) and 30% (right side) height disturbance after using Db6 (top row) and Sym8 (bottom row) wavelets

Table 5 Changes for the height parameters during the introduction of the height disturbance and wavelets Db6, Sym8

	Increase/decrease			*r* / %			*p* / %		
	w/o	Db6	Sym8	w/o	Db6	Sym8	w/o	Db6	Sym8
Ssk	∨	∨	∨	100	100	100	92	73	71
Sku	∨	∨	∨	97	96	97	48	35	32
Sa	∧	∧	∧	98	100	100	54	46	47
Sq	∧	∧	∧	99	99	100	51	35	36
Sv	∧	∧	∧	100	100	100	>100	100	>100
Sp	∧	∧	∧	99	96	100	16	23	30
Sz	∧	∧	∧	100	99	100	63	44	56

The introduction of altitude disturbances resulted in stable, well-correlated increases in most of the altitude parameters (Tab. 5). The largest increase in value was recorded for *Sv*, and the smallest for *Sp*. The measure of the skewness *Ssk* also changed dynamically, approaching 0, which is tantamount to the equalization of the share of valley ordinates and elevations. Changes in the values of all parameters caused by the disturbance decreased with the introduction of wavelets.

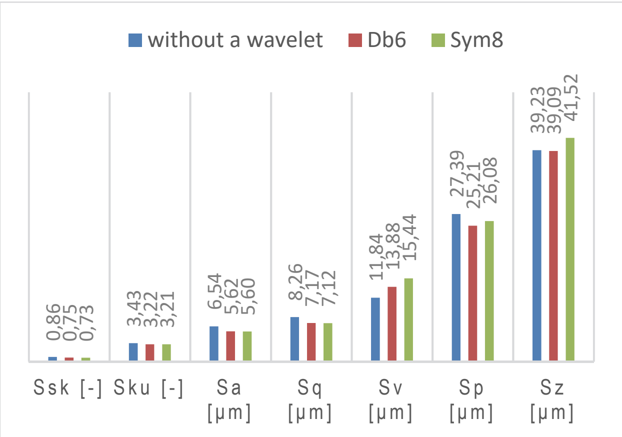

Figure 14 Averaged values of height parameters for surfaces without wavelets and surfaces with wavelets Db6 and Sym8

Fig. 14 shows the change in the average values of individual parameters applying the Db6 and Sym8 wavelets. *Ssk*, *Sku*, *Sa* and *Sq* slightly decrease due to the introduction of wavelets, while the average values of these parameters do not show any noticeable differences between Db6 and Sym8. Larger differences occur in the case of indicators directly referring to the highest elevations and depressions, wherein all three other (*Sv*, *Sp*, *Sz*) Symlet gave a value greater than Daubechies.

3.4 Length Disturbance

The last disturbance, length, brought the biggest changes to the appearance of the surface. Reaching the maximum value of the disturbance (30%), the traces were completely deformed, and only individual peaks retained their original shape. There is also a visible place where no cutting took place due to the occurrence of a large tool shift (Fig. 15).

As in the previous cases, the greatest changes caused by the action of wavelets occurred in the areas of valleys between individual inclines (Fig. 16). Minor surface irregularities were leveled out, but the distribution and shape of the remaining elevations did not improve.

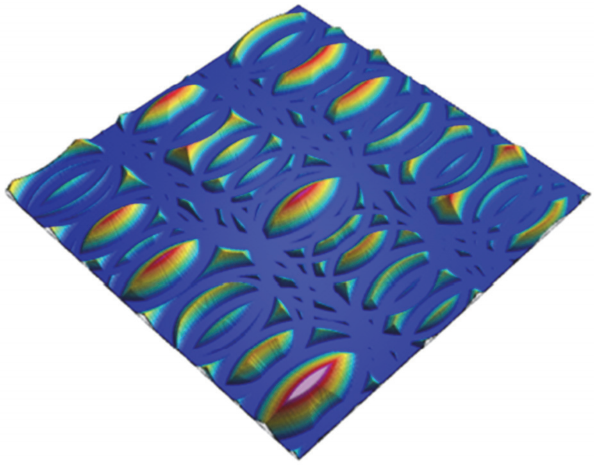

Figure 15 Surface with a 30% length disturbance (area 4 × 4 mm, highest point *Sp* = 44,49 μm, lowest point *Sv* = 5,51 μm)

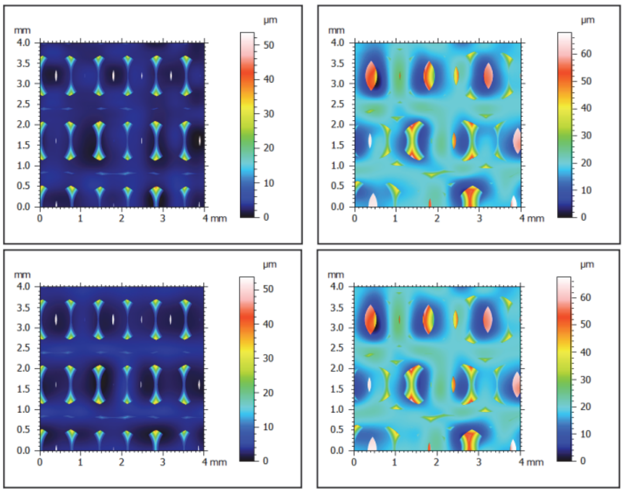

Figure 16 Surface images with 5% (left side) and 30% (right side) lenght disturbance after using Db6 (top row) and Sym8 (bottom row) wavelets

The length disturbance introduced the most unregulated changes occurring when increasing the percentage of disturbance and introducing wavelets (Tab. 6).

The way of changing the values of given parameters in most cases was not established; in a few cases, after the initial increase of a given value with the introduction of a small percentage of disturbance, a given parameter began to decrease again when introducing a larger disturbance (∧/∨). Part of the courses changed around 20% of the disturbance. At this point, inequalities began to appear / the increase in value often stopped / or began to decline.

Table 6 Changes for the height parameters during the introduction of the length disturbance and wavelets Db6, Sym8

	Increase/ decrease			*r* / %			*p* / %		
	w/o	Db6	Sym8	w/o	Db6	Sym8	w/o	Db6	Sym8
Ssk	∧	∧/∨	∨/∧	91	47	1	23	46	14
Sku	∧/∨	∧/∨	∨/∧	91	41	74	44	26	27
Sa	∧	∧/∨	∧	91	16	96	31	18	24
Sq	∧	∧/∨	∧	95	3	98	38	22	28
Sv	∧/∨	∧/∨	∧	89	92	100	30	>100	>100
Sp	∧/∨	∧/∨	∧	94	36	96	77	50	59
Sz	∧	∧/∨	∧	95	72	99	67	67	71

While for the situation without the wavelet and the Sym8 wavelet, courses had single irregularities, which had only a slight impact on the correlation of the results, for the Db6 wavelet, these changes were difficult to unambiguously characterize, and the course of values was often not only increasing or increasing-decreasing. These course changes were more, which influenced the correlation of Db6 parameters and one Sym8, *Ssk* parameter.

An example of a parameter with a disturbed distribution may be *Sv*, which behaves differently for each of the three cases (Tab. 7): in the situation without the wavelet, it takes an inflated value during the initial disturbance introduction (5%), for the wavelet Db6 after the initial increase it decreases for the disturbance maximum (30%), and for the Sym8 wavelet it has a steadily increasing course.

Table 7 Changes for the *Sv* parameter during the introduction of the length disturbance and wavelets Db6, Sym8

Sv / µm	Subsequent values / %						
	0	5	10	15	20	25	30
w/o a wavelet	4,24	4,53	4,38	4,40	4,69	5,12	5,51
Db6	9,13	10,24	11,17	13,07	16,64	20,47	17,17
Sym8	9,91	11,35	12,45	14,37	16,30	18,25	19,90

Sv is also the parameter that changes the most after applying wavelets, which is visible in the graph with averaged values of given parameters for the case of w/o a wavelet, Db6 and Sym8 - Fig. 17.

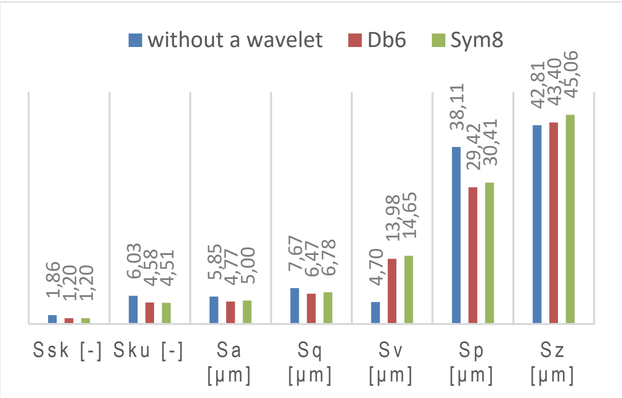

Figure 17 Averaged values of height parameters for surfaces without wavelets and surfaces with wavelets Db6 and Sym8

Apart from *Sv* and *Sz*, all other parameters decrease after applying wavelets. A particularly large decrease in the value can be observed for the maximum height of the peak, *Sp*. The average values of the parameters Db6 and Sym8 differ slightly from each other.

4 CONCLUSIONS

Summarizing the observations presented in point 3, three issues were highlighted:

- The smallest changes after introducing wavelets were observed for noise disturbance, where neither noticeable changes in parameter values nor changes in the waveform with the disturbance increase occurred. This gives information that these wavelets will not work well for this type of modelled surface disturbance. The randomness and small size of the changes in inequality do not allow for proper filtering by the presented wavelets.
- In each case, the action of the wavelets was concentrated in the valley areas, which is confirmed by the surface images and the obtained altitude parameters. In the case of disturbance of the height, most of the parameters after introducing the wavelets reduce the value of the coefficient of the significance of the change *p*, which gives the information that the disturbance has been dampened to some extent.
- In case of disturbances in length, the introduction of wavelets "flattened" the surface, reducing its maximum peak height *Sp* and increasing the height of the greatest depth *Sv*. Some of the irregularities resulting from the disturbance and the shape of the irregularities themselves remained unchanged.
- The application of disturbances and wavelets influenced the values of individual parameters but mostly did not change the shape of the surface.

To summarize, the presented wavelets in milling modelling are the best for reducing height disturbances. Although the presented results did not fully eliminate them, they allow the conclusion that this may be an area for further research. Lack of changes in the general shape of the structure allows replacing the Gaussian filter with wavelets, which allow emphasizing the given surface features, which is visible in the aforementioned changes in parameter values.

Both Sym8 and Db6 cope poorly with minor disturbances in the form of noise. Therefore, if using wavelet analysis in modelling, changes in the entire process should be made.

The operation of both wavelets was very similar. The differences can be seen in the slightly less focused action of the Symlet wavelet. Changes in the appearance of the surface were more subtle, but also they were more stably distributed over the entire area. Whereas, due to its less symmetrical appearance, Db6 showed a tendency to focus on a selected area, which made its action slightly more concentrated. In addition, Db6 turned out to be highly sensitive to length disturbances, small shifts easily changed the value course, which strongly influenced the *r* correlation for this case.

Wavelet analysis in surface modelling is still an area for further research; however, preliminary studies have shown that it is possible to model a mechanically treated surface taking into account any disturbances that may occur in the process, and at least partially visualize whether the wavelet analysis will be able to remove these disturbances from the surface image.

NOMENCLATURE

Db6	mother wavelet Daubechies - order 6
p	significance level
r	correlation level
Sa	arithmetical mean height
Sku	kurtosis
Sp	maximum peak height
Sq	root mean square height
Ssk	asymmetry
Sv	maximum recess depth
Sym8	mother wavelet Symlet - order 8
Sz	maximum height

5 REFERENCES

[1] Khawaja, A. H., Jahanzaib, M., & Cheema, T. A. (2020). High-speed machining parametric optimization of 15CDV6 HSLA steel under minimum quantity and flood lubrication. *Advances in Production Engineering & Management, 15*(4), 403-415. https://doi.org/10.14743/apem2020.4.374

[2] Marusich, T. D. (2001). Effects of friction and cutting speed on cutting force. *ASME MED 23313*, 115-123. https://doi.org/10.1115/IMECE2001/MED-23313

[3] Marusich, T. D., Usui, S., Zamorano, L., Marusisch, K., & Oohnishi, Y. (2010). Improved Titanium Machinig: Modeling and Analysis of 5-Axis Toolpaths via Physics-Based Methods. *Proceedings of 4th CIRP International Conference on High Performance Cutting*.

[4] Marusich, T. D., Thiele J. D., & Brand C. J. (2001). Simulation and analysis of chip breakage in turning processes. *Caterpillar Inc.*, 1-10

[5] Lučić, M., Nedić, B., Marušić, V., Baralić, J., & Mitrović, A. (2020) Analysis of the Temperature Field in the Cutting Zone in Continuous and Discontinuous Metal Cutting by Turning *Tehnicki vjesnik-Technical Gazette*, *27*(5), 1486-1491. https://doi.org/10.17559/TV-20190612173031

[6] Fan W. G., Zhang S., Wang J. D., Wang X. H., Wang W. X. (2020). Temperature Field of Open-Structured Abrasive Belt Rail Grinding Using FEM. *International Journal of Simulation Modelling, 19*(2), 346-356. https://doi.org/10.2507/IJSIMM19-2-CO10

[7] Marusich, T. D., Usui, S., Lankalapalli, S., Saini, N., Zamorano, L., & Grevstad, A. (2006). Residual Stress Prediction for Part Distortion Modeling. *SAE Technical Paper.* https://doi.org/10.4271/2006-01-3171

[8] Strenkowski, J. S. & Carroll, J. T. (1985). A Finite Element Model of Orthogonal Metal Cutting. *Journal of Engineering for Industry*, *107*, 349-354. https://doi.org/10.1115/1.3186008

[9] Strenkowski, J. S. & Athavale, S. M. (1997). A Partially Constrained Eulerian Orthogonal Cutting Model for Chip Control Tools. *Journal of Manufacturing Science*, *119*, 349-354. https://doi.org/10.1115/1.2836809

[10] Ortiz, M. & Quigley, J. J. (1991). Adaptive Mesh Refinement in Strain Localization Problems. *Computer Methods in Applied Mechanics and Engineering*, *90*(1-3), 781-804. https://doi.org/10.1016/0045-7825(91)90184-8

[11] Marusich, T. D. & Ortiz, M. (1995). Modelling and simulation of high-speed machining. *International Journal for Numerical Methods in Engineering*, *38*, 3675-3694. https://doi.org/10.1002/nme.1620382108

[12] ISO 25178: Geometric Product Specifications (GPS) - Surface texture: areal

[13] Kowalski, M., (2005). *Metodyka wyboru parametrów chropowatości do opisu topografii powierzchni*. Politechnika Wrocławska, PhD thesis.

[14] Cichosz, P., Kowalski, M., & Kuzinovski, M. (2003). Modelowanie matematyczne powierzchni szlifowanych obwodowo i czołowo. *Łódź. XXVI Naukowa Szkoła Obróbki Ściernej.*

[15] Cichosz, P., Kowalski, M., & Kuzinovski, M. (2004). Matematicko modelirane na topografijata na deterministicki povrsini. *Conference proceedings*, 106-111.

[16] Cichosz, P., Kowalski, M., & Kuzinovski, M. (2004). Matematicko modelirane na topografijata na stochasticki povrsini. *Conference proceedings*, 112-117.

[17] Cichosz, P. & Kowalski, M. (2004). Modelowanie matematyczne topografii powierzchni płasko wierzchołkowych typu "plateau". *XXVII Naukowa Szkoła Obróbki Ściernej. Zeszyty Naukowe Wydziału Mechanicznego, Politechnika Koszalińska*, 195-202.

[18] Wang, X., Shi, T., Liao, G., Zhang, Y., Hong, Y., & Chen, K. (2017). Using wavelet packet transform for surface roughness evaluation and texture extraction. *Sensors*, *17*(933). https://doi.org/10.3390/s17040933

[19] Brown, C. A., Hansen, H. N., Jiang, X., Blateyron, F., Berglund, J., Senin, N., Bartkowiak, T., Dixon, B., Le Goic, G., Quinsat, Y., Stemp, W. J., Thompson, M. K., Ungar, P. S., & Zahouani, H., (2018). Multiscale analyses and characterizations of surface topographies. *CIRP Annals-Manufacturing Technology, 67*, 839-862. https://doi.org/10.1016/j.cirp.2018.06.001

[20] Gogolewski, D., Makieła, W., Stępień, K., Zmarzły, P., & Wrzochal, M. (2018). The assessment of wavelet transform parameters regarding its use in 3d surface filtering. *29th DAAAM International Symposium*, 1191-1196. https://doi.org/10.2507/29th.daaam.proceedings.172

[21] Gogolewski, D. & Makieła, W. (2021). Problems of Selecting the Wavelet Transform Parameters in the Aspect of Surface Texture Analysis. *Tehnicki vjesnik - Technical Gazette*, *28*(1), 305-312. https://doi.org/10.17559/TV-20190312141348

[22] Karolczak, P. (2021). Application of Discrete Wavalet Transform to Analysis of Cutting Forces in Turning of Composites based on Aluminium Alloys Reinforced with Al_2O_3 Fibres. *FME Transactions*, *49*, 563-574. https://doi.org/10.5937/fme2103563K

[23] Kowalski, M., Kołodziej, M., & Skowronek, H. (2019). Possibilities of using a wavelet transformto assess the surface conditions of abrasives belts. *Mechanik*, *92*(10), 658-60. https://doi.org/10.17814/mechanik.2019.10.87

[24] Hadaś-Dyduch, M. (2019). *Falki dyskretne.* CeDeWu publisher.

[25] Wieczorowski, M. (2009). *Wykorzystanie analizy topograficznej w pomiarach nierówności powierzchni*. Poznań, Wydawnictwo Politechniki Poznańskiej.

[26] Białasiewicz, J., (2004). *Falki i aproksymacje*. Warszawa, Wydawnictwa Naukowo-Techniczne, WNT.

[27] Karolczak, P., Kowalski, M., & Wiśniewska, M. (2020). Analysis of the Possibility of Using Wavelet Transform to Assess the Condition of the Surface Layer of Elements with Flat-Top Structures. *Machines*, *8*(4), 1-21. https://doi.org/10.3390/machines8040065

[28] Dobrowolski, A. & Tomczykiewicz, K. (2008). Analiza falkowa potencjałów czynnościowych jednostek ruchowych. *WAT newsletter*, *LVII*(2), 55-71.

Contact information:

Katarzyna RASZKA, MSc
(Corresponding author)
Wroclaw University of Science and Technology,
Faculty of Mechanical Engineering,
ul. Wyb. Wyspianskiego 27,
50-370 Wroclaw, Poland
E-mail: katarzyna.raszka@pwr.edu.pl